Dependence on quantum confinement of the in-plane effective mass in $Ga_{0.47}In_{0.53}As$/InP quantum wells

C. Wetzel, Al. L. Efros, A. Moll, and B. K. Meyer
Physikdepartment E16, Technical University of Munich, D-8046 Garching, Federal Republic of Germany

P. Omling
Department of Solid State Physics, University of Lund, Box 118, S-221 00 Lund, Sweden

P. Sobkowicz
Institute of Physics, Polish Academy of Sciences, Al. Lotnikow 32/46, 02-668 Warsaw, Poland
(Received 20 November 1991; revised manuscript received 16 March 1992)

Experimental data obtained on undoped, $Ga_{0.47}In_{0.53}As$/InP, single quantum wells using the far-infrared, optically-detected cyclotron resonance technique show a strong increase of the in-plane effective mass of electrons with increasing quantum confinement. The experimental results are compared with a model calculation in which conduction-band nonparabolicity and wave-function penetration into the barrier material have been taken into account. The roughness of the surface between the quantum well and the barrier material is proposed to be the reason for the decrease in electron scattering time from 1.1 ps (1000 Å) to 120 fs (80 Å).

The concept of effective mass is fundamental in the description of semiconductor properties. In two-dimensional (2D) systems, such as a 2D electron gas (2DEG), at heterointerfaces or in quantum wells (QW's) in direct-band-gap semiconductors of $Al_xGa_{1-x}As$/GaAs or $Ga_yIn_{1-y}As$/InP, the electron mass is divided into a mass $m_\perp^*$ perpendicular with respect to the growth plane, and a mass $m_\parallel^*$ parallel to it.[1] Due to the isotropy of m^* in bulk materials, both $m_\perp^*$ and, especially, $m_\parallel^*$ are often approximated by the bulk values.[2] The usefulness of this approximation, however, rapidly decreases as the quantization effects increase. It is known, for instance, that in QW's $m_\perp^*$ increases with increasing subband index.[3] It has also been predicted that as a result of the nonparabolicity of the conduction band, the in-plane mass $m_\parallel^*$ should increase as the thickness of the QW decreases.[3,4]

The experimental verification of these effects is of importance, since the in-plane effective mass is used in many calculations and analyses of other semiconductor properties. So far, the experimental work has been focused on the $Al_xGa_{1-x}As$/GaAs system. Several experimental techniques, direct as well as indirect, have been applied,[5–8] and the results show a small increase of the in-plane effective mass in reasonable agreement with theory. However, a drawback of the direct techniques (e.g., far-infrared absorption) is that, due to low sensitivity, the 2D systems must be heavily doped. This gives an uncertainty in the values of the effective mass due to the increased influence of nonparabolicity (band-filling effects).

Here we report direct measurements of the in-plane effective mass of the electron in nominally undoped $Ga_{0.47}In_{0.53}As$/InP single QW's as a function of well thickness, using far-infrared optically detected cyclotron resonance (FIR-ODCR). In the thinnest QW investigated (80 Å), the in-plane mass is found to increase by about 50% compared with the value of m^* in the bulk $Ga_{0.47}In_{0.53}As$ material. These findings are of great importance for, among other things, the evaluation of fundamental transport properties in quantized structures of $Ga_{0.47}In_{0.53}As$.

After a short introduction to the FIR-ODCR technique, the experimental results will be presented and compared with a theoretical calculation that takes into account both nonparabolicity of the conduction band and the discontinuity between InP and $Ga_{0.47}In_{0.53}As$ where the electronic wave function penetrates into the barrier regions.

ODCR measurements using microwaves have been reported by Baranov *et al.* in Ge.[9] Later the technique was applied to bulk and epitaxial materials of GaAs,[10] CdTe,[10,11] GaP,[12] ZnTe,[12] GaSb,[13] AgBr,[14] Si,[15] and $Al_{0.48}In_{0.52}As$.[16] To date the only reported measurement on a 2D system is that on a $Al_xGa_{1-x}As$/GaAs superlattice by Cavenett and Pakulis.[8] In ODCR measurements microwave-induced changes in the photoluminescence (PL) intensity are monitored as a function of magnetic field. The cyclotron resonance signals are observed at magnetic fields such that the microwave quantum equals the difference between two Landau levels ($\omega_c = eB/m^*$). In contrast to the more familiar, optically detected magnetic resonance (ODMR), in which the transitions are induced by the magnetic-field vector of the microwaves,[17] the ODCR transitions are induced by the electric field vector.

A prerequisite for CR measurements is that $\omega\tau \geq 1$, where ω is the angular frequency of the photons and τ is the carrier relaxation time. Except in very pure materials, τ is too small to allow the detection of CR at microwave frequencies. However, as pointed out by Romestain and Weisbuch[10] using the optical detection technique, the carrier relaxation time is increased because the optically generated carriers screen the ionized impurity scattering centers. Thus, the condition $\omega\tau \geq 1$ can be fulfilled at microwave energies, even though most measurements reported so far have been made under conditions for which $\omega\tau \approx 1$, resulting in very broad resonances and low sensitivity. In order to increase the sensitivity further, Wright *et al.*[18] increased ω by using a FIR laser (ω increases $\approx$250 times compared to microwaves at about 10 GHz). These first results, obtained on GaAs, showed very sharp resonances, allowing the detection of several quantum effects. A later study by Moll *et al.*[19] showed similar results in InP, but also the possibility to detect intradefect $1s$-$2p^+$ transitions in both GaAs and InP.

In our study, the experiments are performed on undoped, single QW's of $Ga_{0.47}In_{0.53}As$ which is lattice matched to InP. The thicknesses of the QW's range from 1000 Å (negligible quantum confinement effects) down to 80 Å. The samples were placed in a superconducting magnet (12 T), and illuminated by a He-Ne laser (3 mW) via an optical fiber. The PL signal was collected with the same fiber, dispersed by a 0.22-m, single monochromator and detected using a cooled Ge detector. The light from a CO_2-pumped, FIR laser (Edinburgh), working at 118.83 μm, was mechanically chopped and guided to the sample via a light pipe. The cw power of the FIR laser was 20 mW and the temperature of the sample was 6 K.

A typical PL spectrum of one of the 100-Å $Ga_{0.47}In_{0.53}As$/InP single-QW samples obtained at 4.0 T is shown in Fig. 1(a). The reason for presenting the spectrum obtained at 4 T is to be able to compare it with the optically detected impact ionization (ODII) spectrum presented below, but no principal differences from the zero-field spectrum are observed. The emission consists of one line at 0.834 eV and a weaker line at 0.819 eV. The 0.834 line originates in unresolved contributions from free excitons (X), bound excitons [(D,X), (A,X)] and donor-to-free-hole (D,h) recombinations. The weaker line is due to free-to-acceptor (e,A) and donor-acceptor (D,A) transitions. All quantum wells investigated show similar PL spectra, only shifted in energy according to the respective quantum confinement effects.

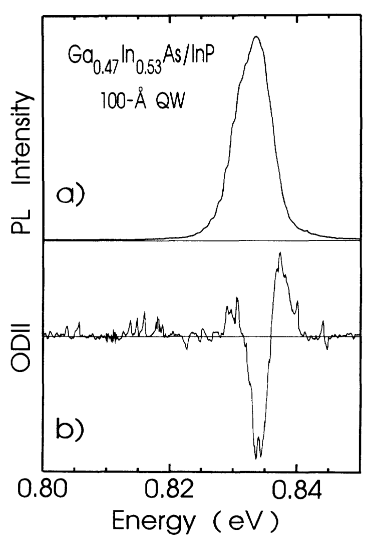

FIG. 1. (a) Photoluminescence spectrum of a 100-Å $Ga_{0.47}In_{0.53}As$/InP QW obtained at a magnetic field of $B=4$ T. (b) The optically detected cyclotron-resonance-induced impact ionization spectrum of the same sample obtained at $B=4$ T using a FIR laser ($\lambda=118.83$ μm). The negative peak at 0.834 eV corresponds to a 0.3% decrease of the photoluminescence line. $T=6$ K.

Figure 2 shows the normalized FIR-induced ODCR signals for 1000-, 200-, 100-, and 80-Å (inset) QW's as observed by monitoring the change in the respective bound-exciton PL intensity as a function of the magnetic field (the peaks correspond to a decrease of the PL). The field positions for the CR signals increase and the peaks become broader as the width of the QW decreases. The values of the change of PL intensity are 5% (1000 Å), 30% (200 Å), 0.4% (120 Å), 0.3% (100 Å), and 0.05% (80 Å). The reason for the large change in the 200-Å sample is not understood, but similar PL changes have been observed in other samples investigated. The values of the in-plane, effective masses of the electrons $m_{\parallel}^*$, determined from these peaks are plotted as a function of the quantum well width in Fig. 3. For the sample with largest resonance width, the effective-mass value is calculated using the magnetic-field value at the estimated peak position, and the uncertainty is calculated from the field positions of half intensity of the peak.

The change in the PL signal induced by the cyclotron resonance (at 4.0 T) as a function of photon energy (ODII) for the 100-Å QW is shown in Fig. 1(b). No spectrum is obtained if we make the detection at a magnetic-field value off the cyclotron resonance. A similar behavior is observed for the other QW's. This clearly shows that the change of the PL intensity is caused by the cyclotron resonance excitation of electrons. From a comparison with the ODCR spectra obtained using microwaves and FIR photons, it was recently shown that the mechanism on which the detection of ODCR is based is cyclotron-resonance-induced impact ionization of the bound excitons and donor-bound electrons.[19] The negative peak at 0.834 eV is, therefore, attributed to such a

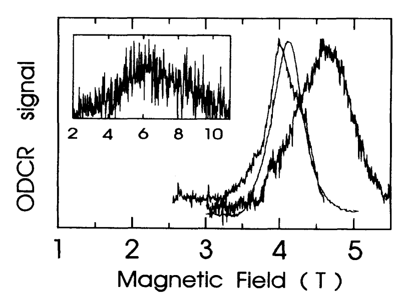

FIG. 2. The FIR-ODCR spectra for the (from low field) 1000-, 200-, 100-, and 80-Å (inset) $Ga_{0.47}In_{0.53}As$/InP QW's. $T=6$ K.

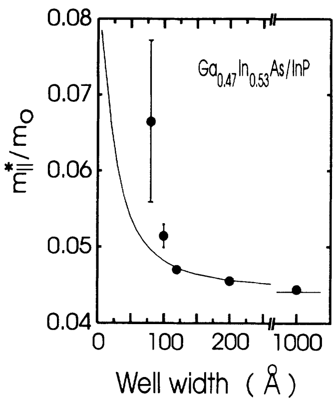

FIG. 3. The measured in-plane effective mass $m_{\parallel}^{*}$ as a function of well width (closed symbols) and the calculated dependence (solid line) using the model described in the text.

decrease of the luminescence due to the impact ionization of bound excitons and donor-bound electrons, and the negative peak at 0.823 eV to a decrease in a (D, A) recombination. The positive peaks are attributed to the increased free exciton (0.837 eV) and (e, A) (0.830 and 0.815 eV) recombinations.

CR measurements of the effective mass are strongly influenced by the doping conditions. Heavy doping results in band filling and as a result the deduced effective-mass values are too high. Due to the high sensitivity of the optical detection method, we were here able to investigate nominally undoped samples, which means that the background doping is in the range $10^{14}-10^{15}$ cm^{-3}. In order to verify the light doping conditions in the QW's, we performed (on the same samples) contactless, microwave-based, Shubnikov–de Haas measurements using a conventional 9-GHz electron-spin-resonance spectrometer.[20] The 2D carrier concentration in the 120-Å QW was found to be 1×10^{11} cm^{-2}, and we conclude that the band-filling effects are very small.

The observed increase of the width of the resonance peaks (see Fig. 2) reflects a decrease in the electron scattering time, τ, from 1.1 ps (1000 Å), 1.2 ps (200 Å), 760 fs (100 Å) to 120 fs (80 Å). Since the procedures used to grow the different quantum wells are identical, there is apparently no reason to attribute this decrease of τ to the material properties. Instead, we believe that it is the increased influence of the surface roughness scattering with decreased well width that is being observed directly. It is interesting to note that the influence of the interface becomes important for QW sizes at which the amplitude of the wave function at the interface is appreciable. This decrease of the scattering time is probably the reason for the failure to detect ODCR in a 60-Å QW of the same material.

The observed increase of the in-plane effective mass with decreasing QW thickness is due mainly to two effects.[4] First, the effective mass increases with electron quantization energy due to the nonparabolicity of the $Ga_{0.47}In_{0.53}As$ conduction band. Second, the effective mass increases as a result of the increased wave-function penetration into the InP barrier material (in which the effective mass of the electron has a value of 0.08 m_0).

In order to describe these effects, we have performed a calculation of the in-plane effective mass for differently sized $Ga_{0.47}In_{0.53}As/InP$ QW's in the envelope-function approximation. In a rectangular, symmetrical QW, the envelope functions of the QW, Ψ_w, and the barriers, Ψ_b, satisfy the standard boundary conditions:

$$\Psi_w\left[\frac{d}{2}\right]=\Psi_b\left[\frac{d}{2}\right],\qquad \frac{1}{m_w^*}\frac{d}{dz}\Psi_w(z)\bigg|_{z=d/2}=\frac{1}{m_b^*}\frac{d}{dz}\Psi_b(z)\bigg|_{z=d/2}, \tag{1}$$

where d is the QW thickness and the z direction is perpendicular to the QW plane. Here we exclude the $k_{\parallel}$-dependent terms[3] because at $k_{\parallel}=0$ they give negligible contributions to the in-plane effective mass. In a three-band Kane model,[21] the energy dependencies of the effective masses, m_w^* and m_b^* are described by

$$\frac{m_0}{m_{w,b}^*(E)}=1+2F_{w,b}+\frac{E_p^{w,b}}{3}\left[\frac{2}{E_g^{w,b}+E}+\frac{1}{E_g^{w,b}+\Delta^{w,b}+E}\right]. \tag{2}$$

Here m_0 is the free-electron mass, $E_g^{w,b}$ the energy gaps, $\Delta_{w,b}$ the spin-orbit splitting of the valence bands, $E_p^{w,b}$ the interband coupling energies, and $F_{w,b}$ the contribution from higher conduction bands. The energy E is defined from the bottom of the conduction bands.

The boundary conditions (1) and Eq. (2) lead to the following equation for the determination of the dispersion law $[E(k_{\parallel})]$ for the lowest 2D subband:

$$\tan\left[\frac{kd}{2}\right]=\frac{kC_wD_w}{\kappa C_bD_b}\frac{2D_b+C_b}{2D_w+C_w}\frac{E_p^b}{E_p^w}. \tag{3}$$

Here ΔE_c is the conduction-band offset,

$$C_w=E+E_g^w,\quad D_w=C_w+\Delta_w,$$
$$C_b=E+E_g^b-\Delta E_c,\quad D_b=C_b-\Delta E_c,$$
$$k^2=\frac{3EC_wD_w}{(E_p^w)^2(2D_w+C_w)}-k_{\parallel}^2,$$
$$\kappa^2=\frac{3(\Delta E_c-E)C_bD_b}{(E_p^b)^2(2D_b+C_b)}+k_{\parallel}^2.$$

Equation (3) and the energy dependencies of the effective masses [Eq. (2)] lead to an expression for the dispersion from which the in-plane effective mass can be calculated:

$$m_{\parallel}^*=\hbar^2/(d^2E/dk_{\parallel}^2). \tag{4}$$

In this way both the effect of nonparabolicity as well as the effect of wave-function penetration into the barrier material are taken into account.

No exact calculation of the nonresonant polaron corrections to the bare electron effective mass has been performed. It is, however, possible to estimate these corrections. For wide wells the electrons can be treated as three dimensional and as originating in the $Ga_{0.47}In_{0.53}As$ well material.[22] The estimated polaron correction is in this case $m_p \approx 1.01m^*$. In the opposite case, that of very narrow QW's, the electron is two dimensional, but a significant part of its wave function resides in the barrier material.[23] The polaron correction is in this case $m_p \approx 1.06m^*$. It has been shown that for a quasi-2D system, many-polaron effects will only decrease these corrections.[24] Therefore, the real values of the polaron corrections lie somewhere between the values given above, and do not influence our principal results.

In the calculation of the in-plane effective mass of $Ga_{0.47}In_{0.53}As$ on quantum-well width we used the following parameters for the well material:[25] $E_p^w = 25.4$ eV, $E_g^w = 0.815$ eV, and $\Delta^w = 0.36$ eV. The contribution from the higher conduction bands, $F_w = -3.13$, is chosen to reproduce the effective mass at the bottom of the conduction band, $m_w^* = 0.044m_0$ obtained from our bulklike sample with $L_z = 1000$ Å. For the InP barriers we apply the parameters[26] $E_p^b = 20.4$ eV, $E_g^b = 1.424$ eV, $\Delta^b = 0.11$ eV, and $F_b = -1.24$, which give the InP effective mass $m_b^* = 0.080m_0$. The band offset used is $\Delta E_c = 0.37\Delta E_g = 0.226$ eV. The calculated dependence of m on the quantum-well width is plotted in Fig. 3 (solid line). These calculated values agree with the experimental data for thicker QW's, but for the 80-Å QW the experimental value of the effective mass corresponds to a 50% effective-mass increase, which is substantially larger than that predicted by the model. Several nominally undoped 80-Å samples show the same result.

Our calculations show that the increase of the effective mass is mainly connected to the barrier leakage of the electron wave function in the narrow QW. Nonparabolicity in a zero-width QW with the highest possible confinement energy would result in only a 20% increase of the effective mass. On the other hand, the influence of the barrier leakage is negligible in the 200-Å QW. The discrepancy between the theoretical and the experimental values of the effective masses in the narrow QW's may be connected with an unpredicted large penetration of the wave function into the barrier. However, such penetration cannot be described by the applied boundary conditions [Eq. (3)]. We have no firm explanation for this deviation, but we can probably exclude the possibility of strong band-filling effects, since microwave-detected Shubnikov–de Haas measurements[20] on the nominally undoped 120-Å QW showed that only the first subband was occupied under similar excitation conditions as during the FIR-ODCR measurements.

A self-consistent calculation of the band structure including this low carrier concentration shows only a minor influence. The band bending has its maximum in the center of the broad 200-Å well but is still only 7% of the first quantization energy. For smaller well widths the bending is much smaller. The result is that the influence on the effective mass is small in this broad well and completely negligible in the narrow ones.

In summary, we have investigated the dependence of the in-plane effective mass of the electron in $Ga_{0.47}In_{0.53}As$/InP QW's as a function of QW width. The mass is found to increase substantially for well widths smaller than 200 Å. The data are compared with a model in which the nonparabolicity and the wave-function penetration into the barrier material are taken into account. With decreasing QW width the $Ga_{0.47}In_{0.53}As$/InP interfaces are observed to become important in the electron-scattering mechanisms, and the electron-scattering time falls from 1.1 ps in the 1000-Å material to 120 fs in the thinnest well.

Note added in proof. We have been able to detect FIR-ODCR on an undoped 50-Å QW. The deduced $m^* = 0.058m_0$, i.e., $\approx 10\%$ higher than the theoretical prediction.

This work has been supported by the Swedish Natural Science Research Council, the Swedish Research Council for Engineering Sciences, and the Deutsche Forschungsgemeinschaft under Contract No. ME898/5-1.

[1] See, e.g., G. Bastard, in *Wave Mechanics Applied to Semiconductor Heterostructures* (Les Édition De Physique, JOUVE, Paris, 1988).

[2] For most practical purposes, the lowest conduction band of $Al_xGa_{1-x}As$/GaAs and $Ga_yIn_{1-y}As$/InP can be regarded as isotropic. However, small anisotropies of the conduction bands have been observed; see, e.g., M. A. Hopkins, R. J. Nicholas, P. Pfeffer, W. Zawadzki, D. Gauthier, J. C. Portal, and M. A. DiForte-Poisson, Semicond. Sci. Technol. **2**, 568 (1987), and references cited therein.

[3] G. Bastard, J. A. Brum, and R. Ferreira, in *Solid State Physics*, edited by H. Ehrenreich and D. Turnbull (Academic, New York, 1991), Vol. 44, p. 229.

[4] U. Ekenberg, Phys. Rev. B **40**, 7714 (1989).

[5] H. L. Störmer, R. Dingle, A. C. Gossard, W. Wiegmann, and M. D. Sturge, Solid State Commun. **29**, 705 (1979).

[6] D. C. Rogers, J. Singleton, R. J. Nicholas, and C. T. Foxon, in *High Magnetic Fields in Semiconductor Physics*, edited by G. Landwehr, Springer Series in Solid-State Sciences Vol. 71 (Springer-Verlag, Berlin, 1987), p. 223.

[7] M. Potemski, J. C. Maan, K. Ploog, and G. Weimann, Solid State Commun. **75**, 185 (1990).

[8] B. C. Cavenett and E. J. Pakulis, Phys. Rev. B **32**, 8449 (1985).

[9] P. G. Baranov, Yu. P. Veshchunov, R. A. Zhitnikov, R. A. Romanov, and Yu. G. Shreter, Pis'ma Zh. Eksp. Teor. Fiz. **26**, 369 (1977) [JETP Lett. **26**, 249 (1977)].

[10] R. Romestain and C. Weisbuch, Phys. Rev. Lett. **45**, 2067 (1980).

[11] Le Si Dang, G. Neu, and R. Romestain, Solid State Commun. **44**, 1187 (1982).

[12] I. J. Booth and C. F. Schwerdtfeger, Solid State Commun. **55**, 817 (1985).

[13] G. R. Johnson, B. C. Cavenett, T. M. Kerr, P. B. Kirby, and C. E. C. Wood, Semicond. Sci. Technol. **3**, 1157 (1988).

[14]I. J. Booth and C. F. Schwerdfeger, Phys. Status Solidi B **130**, 749 (1985).
[15]E. J. Pakulis and G. A. Northrop, Appl. Phys. Lett. **50**, 1672 (1987).
[16]M. G. Wright, A. Kana'ah, B. C. Cavenett, G. R. Johnson, and S. T. Davey, Semicond. Sci. Technol. **4**, 590 (1989).
[17]For a more detailed description of the ODMR technique, see, e.g., B.C. Cavenett, Adv. Phys. **30**, 4 (1981).
[18]M. G. Wright, N. Ahmed, A. Koohian, K. Mitchell, G. R. Johnson, B. C. Cavenett, C. R. Pidgeon, C. R. Stanley, and A. H. Kean, Semicond. Sci. Technol. **5**, 438 (1990).
[19]A. Moll, C. Wetzel, B. K. Meyer, P. Omling, and F. Scholz, Phys. Rev. B **45**, 1504 (1992).
[20]P. Omling, B. K. Meyer, and P. Emanuelsson, Appl. Phys. Lett. **58**, 931 (1991).
[21]E. O. Kane, J. Phys. Chem. Solids **1**, 249 (1957).
[22]H. Fröhlich, H. Pelzer, and S. Zienau, Philos. Mag. **41**, 221 (1950).
[23]S. Das Sarma, Phys. Rev. Lett. **52**, 859 (1984).
[24]F. M. Peeters, Wu Xiaoguang, and J. T. Devresee, Surf. Sci. **196**, 437 (1988), and references cited therein.
[25]S. I. Kokhanovskii, Yu. M. Makushenko, R. P. Seisyan, Al. L. Efros, T. V. Yazeva, and M. A. Abdullaev, Fiz. Tekh. Poluprovodn. **25**, 493 (1991) [Sov. Phys. Semicond. **25**, 298 (1991)].
[26]*Semiconductors,* edited by O. Madelung, M. Schultz, and H. Weiss, Landolt-Börnstein, New Series, Vol. III/17a (Springer-Verlag, Berlin, 1985).